Chemical Physics 501 (2018) 46–52

Contents lists available at ScienceDirect

Chemical Physics

journal homepage: www.elsevier.com/locate/chemphys

Monolayer adsorption of noble gases on graphene

Sidi M. Maiga, Silvina M. Gatica *

Department of Physics and Astronomy, Howard University, 2355 Sixth St NW, Washington, DC 20059, USA

ARTICLE INFO

Article history:
Received 15 August 2017
In final form 28 November 2017
Available online 6 December 2017

ABSTRACT

We report our results of simulations of the adsorption of noble gases (Kr, Ar, Xe) on graphene. For Kr, we consider two configurations: supported and free-standing graphene, where atoms are adsorbed only on one or two sides of the graphene. For Ar and Xe, we studied only the case of supported graphene. For the single-side adsorption, we calculated the two-dimensional gas-liquid critical temperature for each adsorbate. We determined the different phases of the monolayers and constructed the phase diagrams. We found two-dimensional incommensurate solid phases for krypton, argon and xenon, and a two-dimensional commensurate solid phase for krypton. For double side adsorption of Kr, we do not see evidence of an ordering transition driven by the interlayer forces.

1. Introduction

The properties of adsorbed monolayers (one-atom thick layer) have been investigated for many years, motivated by the realization of 2D matter and the implications on the new technologies based on new materials. For example, adsorption of noble gases have been studied on many substrates like graphite [1–5] and metals [6–9].

Bruch et al. constructed the phase diagrams of noble gases adsorbed on graphite, by collecting data from several experiments [10]. For monolayer Kr, two solid phases are observed in the diagram: an incommensurate solid (IS) and a commensurate solid (CS) with a fractional coverage of 1/6 (one Kr atom per every 6 carbons). Monolayer Ar and Xe, on the other hand, do not exhibit a 2D-CS phase.

One may expect that the behavior of monolayers on graphene would be qualitatively similar to those on graphite. However, phase transitions may be dramatically affected by the extra carbon layers. Particularly commensurate solid phases, which are extremely sensitive to the corrugation of the substrate, may completely vanish due to a slight change in the force of the substrate.

In Ref. [11], Bruch et al. studied the case of monolayers formed on both sides of a suspended graphene sheet. They conclude that the gas–liquid critical temperature would be less than 10% higher than the value on graphite.

In a recent study Madeira et al. [12] computed the specific heat and melting temperatures of rare gases adsorbed on graphene. Their study was done by molecular dynamics simulations in the canonical ensemble.

We have extensively studied the behavior of Kr and Ar on suspended single-walled carbon nanotubes [13–15], and found that Kr forms a cylindrical shell that has a unique CS structure with fractional coverage 1/4. This 1/4-CS appears exclusively on medium-sized zigzag nanotubes. On larger NTs, Kr forms a shell of coverage 1/6 that is, however, not solid (notice that this coverage corresponds to the usual $\sqrt{3} \times \sqrt{3}\ R\ 30^{\circ}$ phase seen on graphite). For Ar on the other hand we have not observed commensuration in any of the nanotubes tested. These results motivated the present study, having in mind that graphene represents an infinite-radius carbon nanotube.

In this paper we report numerical results of the monolayer adsorption of Ar, Kr and Xe on a graphene sheet. We place the graphene at the bottom of the simulation cell letting adsorption occur on one side only; this case would correspond to a layer of graphene on top of a substrate (or "supported graphene", SG), although our treatment neglects any contribution of the support to the potential energy of the adlayer. For Kr, we also consider the adsorption on free-standing graphene (FSG), where monolayers are formed on both sides. We use the method of Grand Canonical Monte Carlo (GCMC) [16], which has been extensively used for simulations of adsorption [17–19]. We compute the average number of atoms adsorbed on a substrate as a function of the pressure of the vapor and temperature of the system. In the simulations, we collect sample configurations that we use to test the structure of the monolayers. From calculations of the radial distribution function and structure factor we evaluate the phase of the monolayer (liquid, IS or CS). Given that the mass and size of argon, krypton and xenon are large enough to allow a classical treatment, our simulations can

* Corresponding author.
E-mail address: sgatica@howard.edu (S.M. Gatica).

https://doi.org/10.1016/j.chemphys.2017.11.020
0301-0104/

produce adsorption isotherms in a wide range of pressure and temperature. In this way, our findings can be directly compared to experimental results.

2. Methodology

The simulation cell is a rectangular box of base-size 39.35×38.46 Å. The graphene sheet is positioned at the base of the cell ($Z = 0$) for SG, and in the middle of the cell for FSG. The height of the cell is 75 Å for SG and 150 Å for FSG. The boundary conditions were set periodic in the X and Y directions and reflective in Z.

For each gas, simulations were run at several values of the temperature and pressure of the vapor. For Ar, the simulation temperature ranged from 41 K to 79 K at 2 K increments; from 70 K to 140 K with an increment of 5 K for Kr and from 90 K to 160 K at 5 K increments for Xe. Each GCMC simulation was done at fixed temperature (T) and chemical potential (μ); μ is related to the pressure of the vapor in equilibrium with the adsorbate by the equation of state. In our simulations we considered the vapor an ideal gas.

The graphene layer was assumed to be rigid and infinitely wide on the X, Y plane, which we realized by setting periodic boundary conditions on the X, Y directions. The input data of the simulation are the pressure of the vapor (P), and the temperature (T); the output data are the average number of adsorbed atoms (N), the averages of the total energy per particle (E_T), the gas-substrate energy per particle (E_{gs}) and the gas–gas energy per particle (E_{gg}). We also collected samples of the coordinates of the adsorbed atoms. The number of MC moves for each single data point in the isotherms was typically 3 million, to reach equilibrium. Additionally, one million moves were performed for data collection. For each temperature, the simulation was run 90 times; each time, the pressure was increased by 10%. The ratio of creation/deletion/translation moves was set to 0.40/0.40/0.20.

The potential interaction energy between an atom in the gas (adatom) and a carbon atom in graphene was calculated with the anisotropic Lennard Jones (LJ) potential [20]. In the anisotropic potential, the pairwise interaction depends not only on the distance between the carbon atom and the adatom, but also on the angle (θ) between the vector $\vec{r}$ (relative position of the adatom and the carbon atom) and the surface's normal. The potential is given by,

$$U(\vec{r}) = 4\epsilon\left\{\left(\frac{\sigma}{r}\right)^{12}\left[1+\gamma_R\left(1-\frac{6}{5}\cos^2\theta\right)\right] - \left(\frac{\sigma}{r}\right)^{6}\left[1+\gamma_A\left(1-\frac{3}{2}\cos^2\theta\right)\right]\right\}, \quad (1)$$

where ϵ and σ are the LJ parameters; γ_A and γ_R determine the anisotropy of the dispersion potential. This angular dependence originates in the anisotropy of the π bonds of the C atoms in the graphene sheet; as a result the potential becomes more corrugated.

The LJ parameters for the adatom-C potential are obtained by fitting physical properties of the gases [21] and using the semi-empirical Lorentz-Berthelot combining rules: [22] (Table 1)

Table 1
Lennard Jones parameters of the adsorbates and substrate [21].

Adsorbate	ϵ_{aa}(K)	σ_{aa}(Å)
Ar	120.0	3.4
Kr	171.0	3.6
Xe	221.0	4.1
C (graphene)	28.0	3.4

$$\sigma_{aC} = \frac{\sigma_{aa}+\sigma_{CC}}{2} \quad (2)$$

$$\epsilon_{aC} = \sqrt{\epsilon_{aa}\epsilon_{CC}} \quad (3)$$

We have adopted $\gamma_A = -0.54$ and $\gamma_R = 0.38$ based on a previous study of He on graphite by Cole et al. [20]. The interaction energy between adatoms was calculated with the isotropic LJ potential, given by Eq. (1) with $\gamma_R = \gamma_A = 0$. The LJ potential was truncated at a distance of 5σ.

To determine the phase behavior of the adsorbed monolayers, we inspected the discontinuities or steps in the energy gas-surface function $E_{gs}(P)$ and the adsorption isotherms $N(P)$. We carefully analyzed sample configurations around steps in the isotherms. Based on the radial distribution function, we determined the phase (solid or liquid). Similarly, we evaluated the commensuration i.e. CS or IS based on the structure factor.

The two-dimensional radial distribution function (2D-RDF) $g(r)$ of a system of particles describes how the density varies as a function of the distance from a reference particle. For a distribution of atoms or molecules on a surface, it is given by the following equation:

$$g(r) = \frac{N_r}{2\pi r dr n}, \quad (4)$$

where N_r is the mean number of atoms at distance between r and $r + dr$ from a given atom and n is the number of atoms per unit area.

The structure factor $S(\vec{k})$ characterizes the amplitude and phase of a wave diffracted from crystal lattice planes. It is simply the Fourier transform of the pair correlation function given by,

$$S(\vec{k}) = \frac{1}{N}\left|\sum_j^N \exp\left(i\vec{k}\cdot\vec{R_j}\right)\right|^2, \quad (5)$$

where $\vec{k}$ is the 2D wave vector and $\vec{R_j}$ is the position vector of the j^{th} particle in the monolayer. $\vec{k}$ can be written in terms of the reciprocal lattice vectors $\vec{b_1}$ and $\vec{b_2}$,

$$\vec{k} = m_1\vec{b_1} + m_2\vec{b_2}, \quad (6)$$

with m_1 and m_2 arbitrary real numbers. For a perfect lattice, $S(\vec{k})$ is equal to 1 for all integer m_1 and m_2, and identically zero for non-integer values. On the other hand, $S(\vec{k} \neq 0) \ll 1$ for an array of atoms in a non-matching lattice or a non-solid phase.

3. Results

3.1. Argon

Fig. 1 represents the adsorption isotherms $N(P)$ for argon adsorbed on SG. For each temperature, we observe that at low vapor pressure the number of adsorbed atoms is very small ($N \sim 0.001$ Å^{-2}), which corresponds to a 2D gas. At a higher pressure, the density of the film rapidly raises. The lower the temperature the faster the film's density grows. For example, at the lowest temperature seen in Fig. 1 (41 K), the isotherm shows a discontinuous jump to form a film of density 0.0726 Å^{-2}. Vertical steps in the isotherms appear for higher temperatures as well, up to the critical temperature T_c at which the isotherms qualitatively change to smooth continuously growing curves. For temperatures lower than T_c, there is a coexistence of a 2D gas and a dense monolayer, which can be solid or liquid. As the temperature increases, the difference between the gas and monolayer densities decreases approaching zero at $T = T_c$. The critical temperature T_c is computed as the temperature at which the inverse slope of the isotherms approaches zero. The result of our calculation is $T_c = 61$ K ± 1 K.

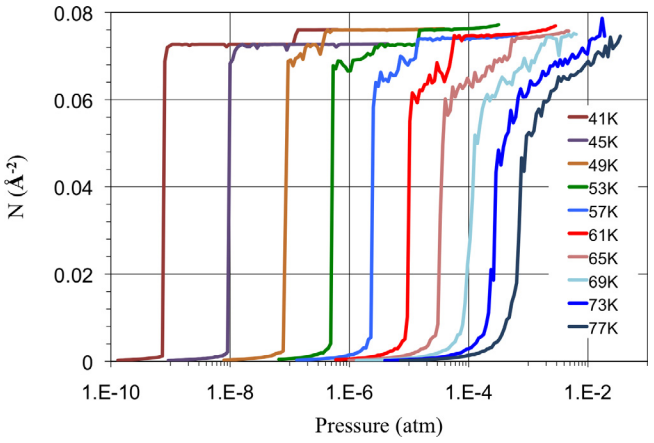

Fig. 1. Adsorption isotherms of Ar on graphene at temperatures from 41 K to 77 K, from left to right.

The critical temperature of a two-dimensional Lennard-Jones lattice has been theoretically predicted to be $T_{c(LJ)} = 0.52\epsilon$ [23]. In the case of Ar it results 62 K, in excellent agreement with our calculation. Experimental measurements of the critical point of monolayer Ar on graphite are $T_c = 59$ K [4] and 55 K [3], which are 3 and 10% lower than our prediction.

By inspecting the adsorption isotherms, the 2D-RDF and the structure factor of several samples in the monolayer regime we determined the phases (G, L, IS or CS). At the lowest temperatures, the density remains constant for a wide range of pressures, seen as the flat portion of the isotherm. At higher vapor pressure, the monolayer slightly compresses from 0.0726 to 0.076 Å^{-2}. In this regime, the argon monolayer is an incommensurate solid. At higher temperature, on the other hand, the monolayer is a 2D liquid transitioning to a 2D IS. Hence, for Ar we found three phase transitions: 2D-G to 2D-L, 2D-G to 2D-IS and 2D-L to 2D-IS.

For comparison, the 2D-density of the commensurate solid phase on graphene or graphite, which has a ratio 1/6 adsorbate/-carbon atoms is 0.063 Å^{-2} while the 2D-LJ solid lattice has a density 0.079 Å^{-2}. In our simulation, we obtained a monolayer of density 0.0726–0.076 Å^{-2}, consistent with an incommensurate solid phase.

Our results are summarized in a phase diagram, shown in Fig. 2, where we see three coexistence lines: G-IS and G-L and L-IS. We estimated the triple point temperature at $T_t = 47$ K ± 1 K. This value is in excellent agreement with the experimental report for Ar on graphite from Migone et al. [3] ($T_t = 47$ K) and in fair agreement with the result of D'Amico et al. [1] ($T_t = 49.7$ K).

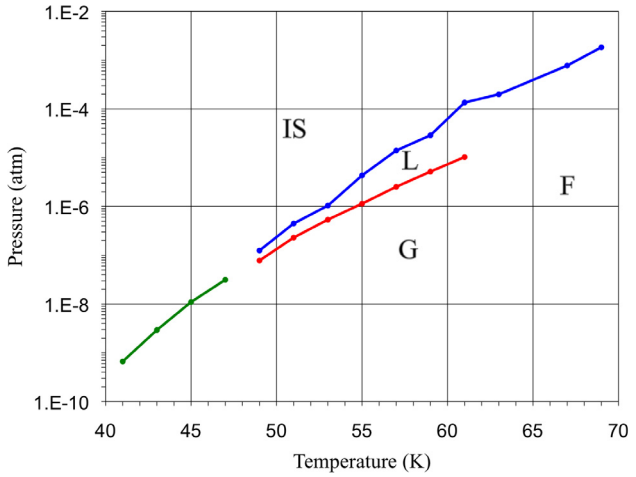

Fig. 2. Phase diagram of monolayer Ar on graphene. The labels indicate incommensurate solid (IS), liquid (L), gas (G) and fluid (F) phases.

3.2. Krypton

We first studied the single-side monolayer adsorption of Kr on SG. The adsorption isotherms for few temperatures are shown in Fig. 3. Using the same analysis as in the argon case, we estimated a 2D G-L critical temperature $T_c = 90$ K ± 5 K, which agrees with the theoretical value $T_{c(LJ)} = 89$ K and is 5% higher than the experimental result reported in Ref. [4] (85.3 K).

The density of the Kr solid monolayer at 80 K varies from 0.065 to 0.075 Å^{-2}. The values are consistent with a 1/6 CS (density 0.063 Å^{-2}) that is compressed to an IS 2D-LJ lattice (density 0.071 Å^{-2}). Hence, contrary to the case of Ar, Kr forms both commensurate and incommensurate solid phases. The CS phase is observed at low temperature and low pressure, while the IS appears at higher P and T.

To illustrate our analysis, in Fig. 4 we show the adsorption isotherms, gas-surface energy, 2D-RDF and SF at 80 K and 95 K. At both temperatures we notice large fluctuations in the monolayer density suggesting a change of phase. Although the 2D-RDF in both cases is consistent with a solid phase, there is a qualitative distinction in the gas-substrate energies, also shown in Fig. 4: at 80 K and as the vapor pressure reaches $P = 1.73 \times 10^{-5}$ atm, the energy gas-substrate suddenly decreases by 0.1 kJ/mol (12 K), suggesting the formation of a CS arrangement; at 95 K, on the other hand, the E_{gs} is a monotonic function of the pressure, apart from statistical fluctuations.

The structure factor ($S(\vec{k} = m_1\vec{b_1} + m_2\vec{b_2})$) is shown as a function of m_1 (with $m_2 = 0$). At $T = 95$ K the SF is mostly flat, meaning that the phase is IS. At $T = 80$ K, on the other hand, the SF shows a pick at $m_1 = 1$, indicating a structure consistent with a CS phase.

We examined the case of $T = 80$ K in more detail. We observe that the monolayer forms at a vapor pressure $P = 1.6 \times 10^{-5}$ atm, accompanied by a sudden increase in the magnitude of the E_{gg} to reach 3.92 kJ/mol (472 K), as seen in Fig. 5. The CS structure formed at higher pressure is clearly noted in the average 2D density at $P = 1.16 \times 10^{-4}$ atm, shown in Fig. 6.

From this analysis we identified transitions 2D-G to 2D-L, 2D-G to 2D-CS, 2D-L to 2D-CS and 2D-F to 2D-IS, represented in Fig. 7. According to our results there is a triple point at temperature $T_t = 75$ K ± 5 K.

We next run simulations of Kr adsorption on FSG, where adsorption takes place on both sides of the graphene layer. Results are shown in Fig. 8. As in the case of single-side adsorption, the E_{gs}

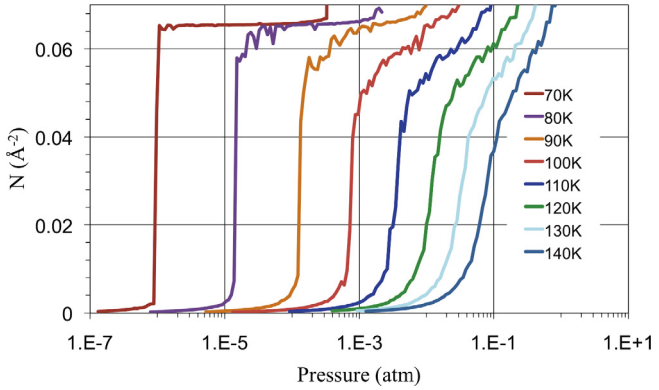

Fig. 3. Adsorption isotherms of Kr on graphene at temperatures from 70 K to 140 K, from left to right.

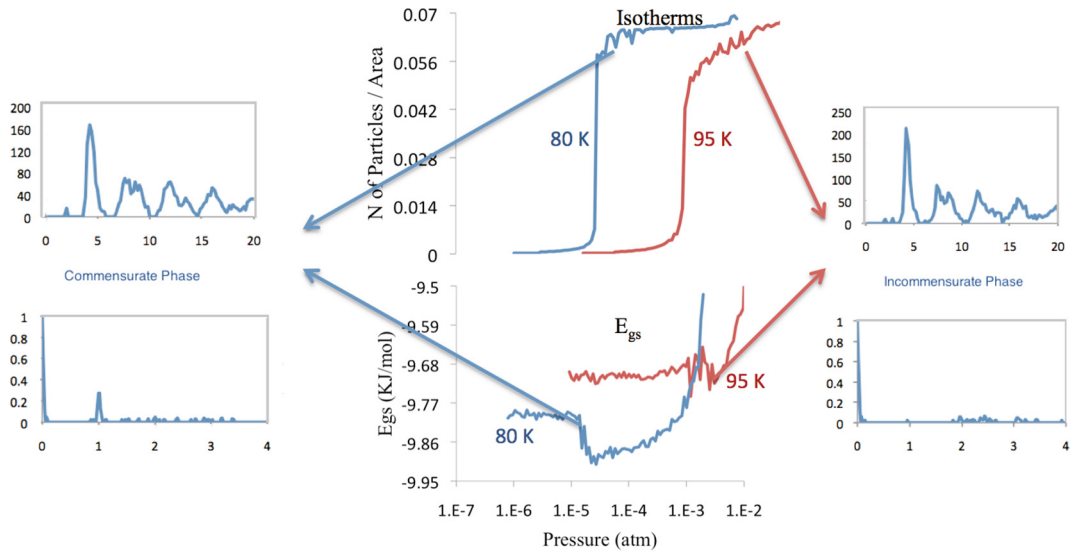

Fig. 4. Center column: Adsorption isotherms (upper) and gas-surface energy (lower) for Kr at 80 K and 95 K. Left and right columns: 2D-RDR (upper) and magnitude of the SF (lower) at 80 K (left) and 95 K (right).

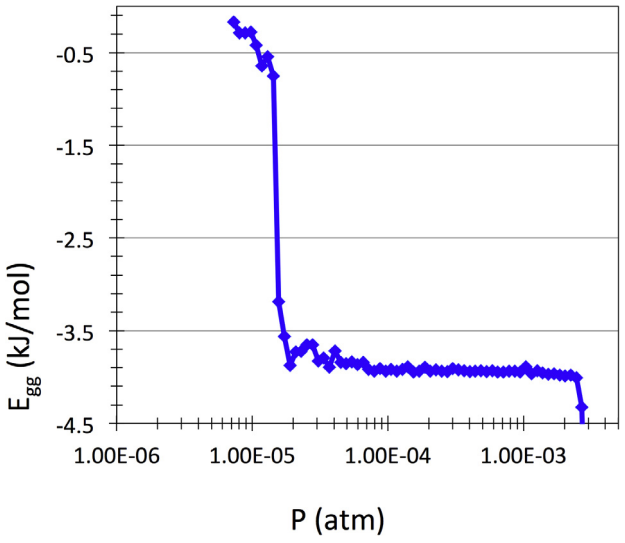

Fig. 5. E_{gg} for Kr on supported graphene at 80 K.

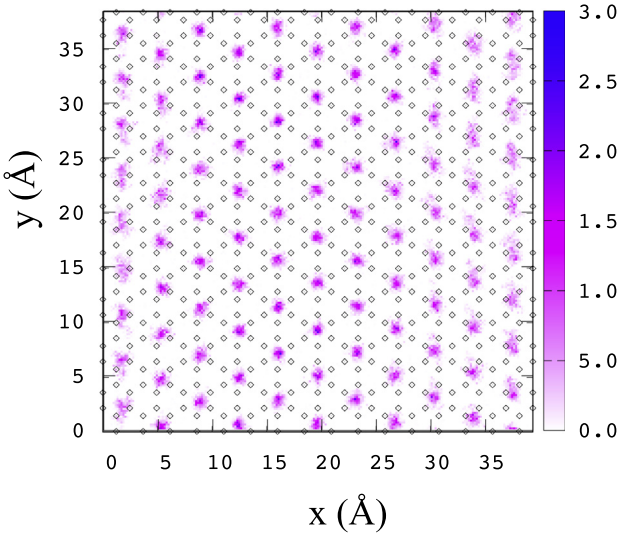

Fig. 6. Monolayer density (in Å^{-2}) for Kr on supported graphene at 80 K and $P = 1.16 \times 10^{-4}$ atm. Also shown are the carbon atoms (black diamonds).

decreases by 0.1 kJ/mol at a $P = 1.7 \times 10^{-5}$ atm, indicating the formation of a CS. However the monolayer is formed at a slightly lower pressure ($P = 1.4 \times 10^{-5}$ atm), with E_{gg} of magnitude 4.15 kJ/mol (500 K). The E_{gg} difference between single and double sided adsorption is 28 K, which corresponds to the inter-layer Kr-Kr energy.

The 2D density is shown in Fig. 9 at T = 80 K and pressures 1.6×10^{-4} to 7.82×10^{-4} atm. The figures display the overlapping of two CS patterns on each side of the graphene. We believe there is no correlation between the two Kr layers, since the Kr-Kr energy (E_{gg} in Fig. 8) does not reflect changes that would indicate an ordering transition.

3.3. Xenon

Finally, we simulated the single-side monolayer adsorption of xenon on SG. We run simulations from T = 90 K to T = 160 K. A few adsorptions isotherms are represented in Fig. 10. Our calculation of the 2D G-L critical temperature is $T_c = 115$ K ±5 K, which coincide with the theoretical value, $T_{c(LJ)} = 115$ K and the experimental value for Xe on graphite, 117 K [5].

The monolayer density in the simulation is 0.057 Å^{-2}, which is lower than the value of the commensurate solid phase (0.063 Å^{-2}) and similar to the LJ solid lattice (0.055 Å^{-2}). From the inspection of the 2D-RDF and SF we observed transitions from gas and liquid phases to an incommensurate solid phase.

We exhibit the resulting phase diagram in Fig. 11. We find a triple point at $T_t = 100$ K ±5 K, in agreement with the experimental value for Xe on graphite (99 K [5]).

4. Comparison with graphite

As expected, the adsorption starts at a higher pressure on graphene than on graphite, due to the attraction of the extra layers in the later. We can estimate the excess substrate energy exerted by graphite by comparing the low-coverage pressure or chemical

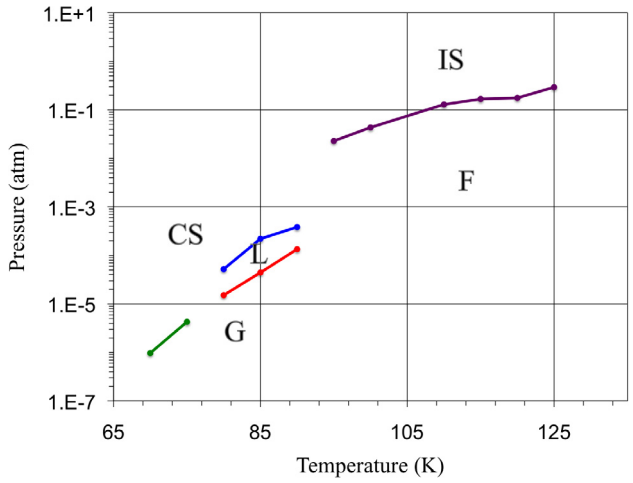

Fig. 7. Phase diagram of monolayer Kr on graphene. The labels indicate incommensurate solid (IS), commensurate solid (CS), liquid (L), fluid (F) and gas (G) phases.

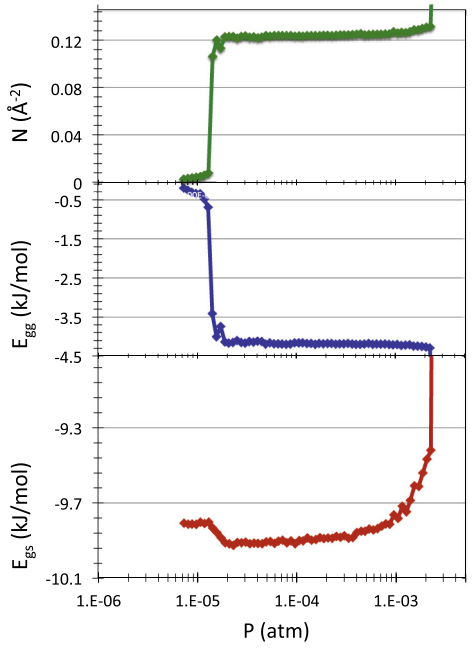

Fig. 8. Double-side adsorption isotherm N (top), E_{gg} (middle) and E_{gs} (bottom) for Kr on free standing graphene at 80 K.

potential of adsorption. To do so, we write the chemical potential of the adsorbed monolayer as,

$$\mu_{ads} = -E_S + k_B T \ln(n\lambda^2), \tag{7}$$

where $\lambda = \sqrt{h/(2\pi m k_B T)}$ is the thermal wavelength and we assume that the adsorbate is a two-dimensional monolayer of number density n.

Assuming that the density of the monolayer is equal on both substrates, we can estimate the excess energy by the difference in the chemical potentials at the same temperature,

$$\Delta E = E_{graphite} - E_{graphene} = -(\mu_{graphite} - \mu_{graphene}) \tag{8}$$

The chemical potential can be obtained by noting that since the adsorbate is in equilibrium with the vapor, the chemical potentials of each phases are equal,

$$\mu_{ads} = \mu_{vapor} = k_B T \ln(\lambda^3 P/(k_B T)), \tag{9}$$

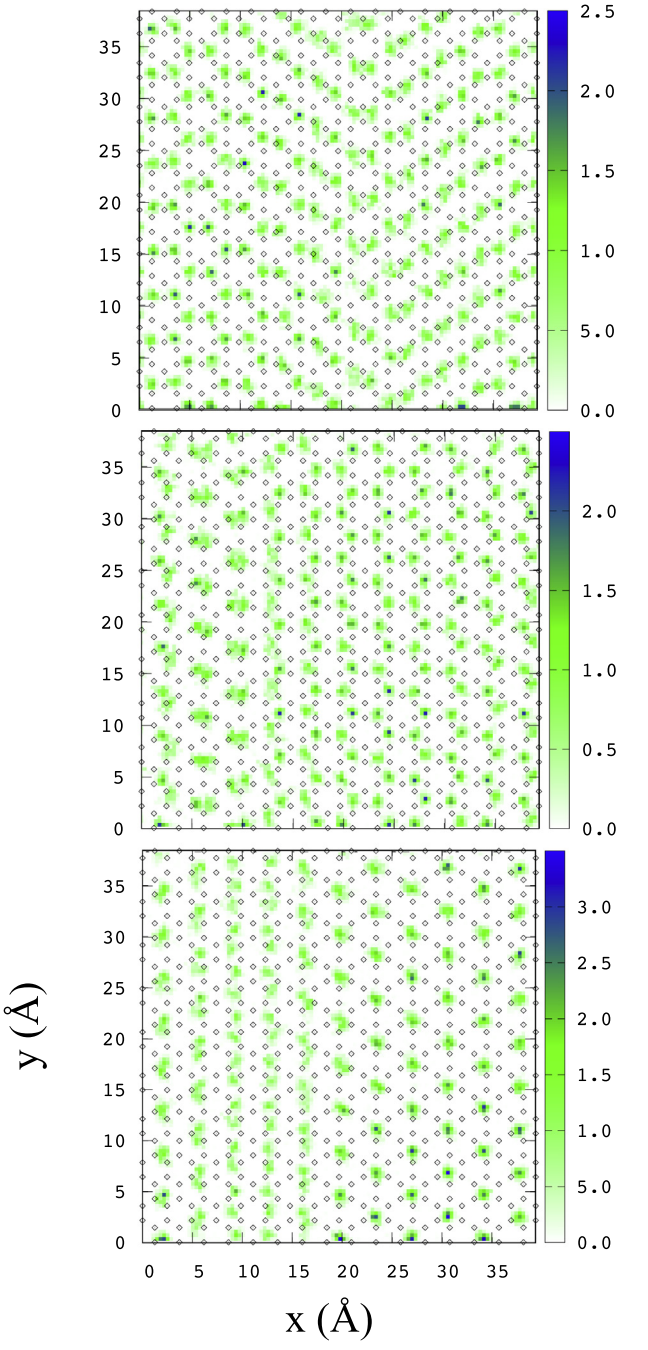

Fig. 9. Monolayer density (in Å^{-2}) for Kr on free standing graphene at 80 K and $P = 1.16 \times 10^{-4}$ atm (top), $P = 3.01 \times 10^{-4}$ atm (middle) and $P = 7.81 \times 10^{-4}$ atm (bottom). Also shown are the carbon atoms (black diamonds).

assuming that the vapor is an ideal gas. We finally obtain,

$$\Delta E = k_B T \ln(P_{graphene}/P_{graphite}). \tag{10}$$

Here $P_{graphene}$ and $P_{graphite}$ are the adsorption pressure on each substrate at equal temperature.

For example, in the case of Ar on graphite, the gas and solid phases coexist at a pressure $P = 1.0 \times 10^{-7}$ torr and temperature $T = 42.3$ K (extracted from Fig. 6.9 in Ref. [24]). From our simulations, the pressure of coexistence at the same temperature is $P = 1.72 \times 10^{-9}$ atm, or 1.3×10^{-6} torr (see Fig. 2). A quick calculation using Eq. 10 gives $\Delta E = 109$ K. This result is within 4% of the

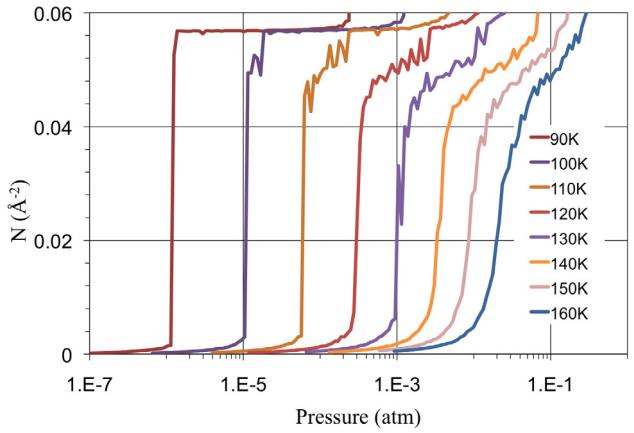

Fig. 10. Adsorption isotherms of Xe on graphene at temperatures from 90 K to 160 K, from left to right.

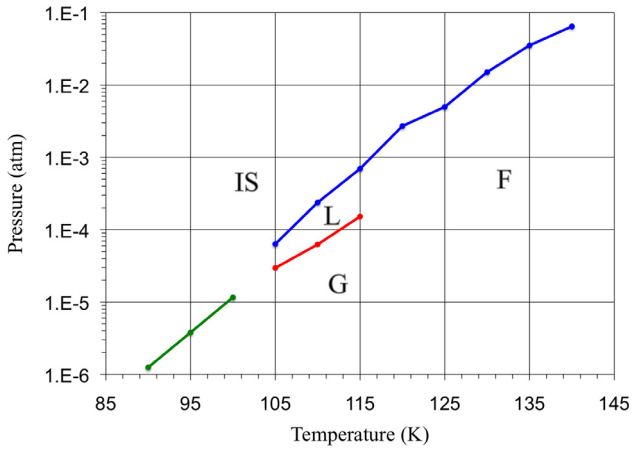

Fig. 11. Phase diagram of monolayer Xe on graphene. The labels correspond to incommensurate solid (IS), liquid (L) gas (G) and fluid (F) phases.

energies reported by Bartolomei et al. [25], where $\Delta E = 9.8$ meV = 113.7 K. Overall, the phase diagram of Ar on graphene (Fig. 2) is qualitatively similar to the graphite counterpart in the monolayer regime. (see Fig. 6.9 in Ref. [24]).

For Kr, the phase diagrams are qualitatively similar in the low-T/low-P regime: a liquid phase is found between 80 and 90 K on graphite (see Fig. 6.12 in Ref. [24]) and in our simulations as well; also, a G-CS coexistence line appears below 80 K in both substrates. Our calculations show a F-IS coexistence line at pressure above 0.01 atm and temperatures from 95 to 125 K, similar to the IC-RF line in the graphite phase diagram. The most significant qualitative difference among both diagrams is that for Kr on graphite the CS phase appears up to a temperature of approximately 130 K, while in our simulations we only found the CS below T = 95 K.

For Kr on graphite, we can roughly estimate that at 80 K the monolayer gas and solid phases coexist at a chemical potential $\mu_{graphite} = -2200$ K (from Fig. 6.12 in Ref. [24]). From our simulations of Kr on graphene, we obtain coexistence at the same temperature and $P = 1.40 \times 10^{-5}$ atm, which corresponds to a chemical potential $\mu_{graphene} = -2008$ K. The difference gives $\Delta E = 191$ K, 20% higher than the value obtained from Ref. [25] ($\Delta E = 151$ K).

5. Summary and conclusions

Using Grand Canonical Monte Carlo simulations, we studied the adsorption of noble gases (argon, krypton and xenon) on a graphene sheet. From the computed adsorption isotherms, we calculated the 2D gas-liquid critical temperature for each gas, resulting in fair agreement with theoretical predictions and experimental values of monolayers on graphite. We determined the phases of the adsorbed monolayers by inspecting the radial distribution function and the structure factors, and constructed the phase diagrams in the P-T plane. We found 2D incommensurate solid phases for krypton, argon and xenon on graphene, and a 2D commensurate solid phase for krypton at low temperature. In Ref. [12] the authors report the melting temperatures 56.0 K, 107.9 K and 175.3 K for Ar, Kr and Xe respectively, at the 1/6-CS density (0.063 Å^{-2}). Since the values of the chemical potential are not given, we can not make a rigurous comparison but we note that their melting temperatures for Ar and Kr coincide with our findings at approximately $P = 1.0 \times 10^{-5}$ and 0.1 atm respectively; the melting temperature reported for Xe is out of the range of our simulations. They also found a CS phase for Kr and IS phases for Ar and Xe, in agreement with our findings.

The absence of a commensurate solid phase in the case of Xe is simply caused by its size: Xe does not "fit" in the 1/6 lattice. On the other hand, the qualitative difference between the behavior of Kr and Ar is due to a combination of size and energy effects that make the corrugation slightly higher for Kr. The corrugation of the potential is defined as the energy difference between the least attractive and the most attractive sites on the surface. Those sites are shown in Fig. 12. The most attractive site is on top of the center of a hexagon, and the least attractive sites are both on top of a carbon atom or on top of a bridge. The corrugation is 56.7 K for Kr and 54.9 K for Ar (see Fig. 13). These values differ in only 2 K (3%)! The size of the atoms is also quite similar: Kr is only 6% larger than Ar. However, Kr seems to have the right size to form a commensurate solid on graphene while almost matching the density of the 2D LJ incommensurate solid, hence doubling the energy rewards.

The main approximations used in our simulations are that the graphene layer is rigid, the substrate supporting the graphene is ignored, the vapor in equilibrium with the adsorbate is assumed to be an ideal gas, and the carbon-adatom interaction parameters are calculated using empirical combining rules. In spite of these approximations, the comparison with other available studies is good. The theoretical predictions of the 2D-LJ critical temperature coincide with our values. The experimental measurements of the critical temperatures agree with our values for Xe, and are 5% and 3–10% lower for Kr and Ar respectively. These diferences suggest that the substrate sligtly affects the behavior of the 2D monolayer, being Ar the most affected and Xe the least. This trend follows the relative strength of the substrate given by the ratio $\epsilon_{gs}/\epsilon_{gg}$, which is 0.48, 0.40 and 0.35 for Ar, Kr and Xe respectively.

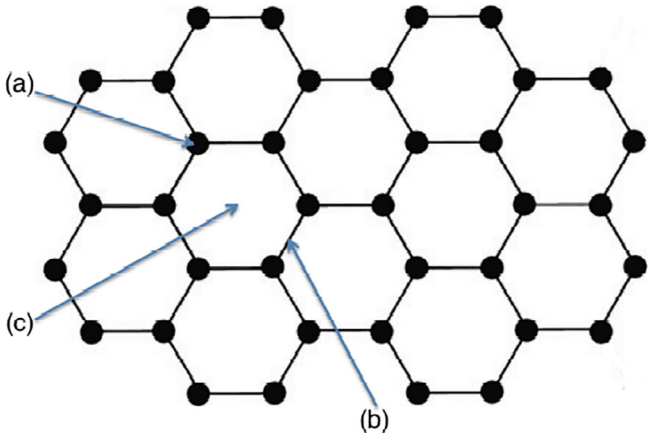

Fig. 12. Three different adsorption sites on top of graphene: *above* (a), *bridge* (b) and *center* (c).

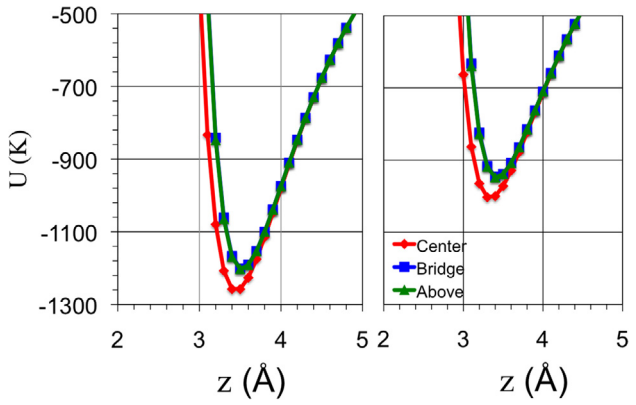

Fig. 13. Adsorption potentials of Kr (left) and Ar (right) at a distance z on top of *above*, *bridge* or *center* sites. The first two curves overlap.

We compared the phase diagrams of Ar and Kr on graphene with the ones on graphite. We found that for Ar or Kr on graphene, the coexistence lines are qualitatively similar and shifted to higher pressures as expected due to the attractive extra carbon layers in graphite. However for Kr on graphene, the CS phase only appears below 95 K, while on graphite it is seen up to 130 K. This difference may be explained by an enhanced corrugation on graphite, alghough to be conclusive we should run simulations on graphite with the same method and potential model.

We also simulated the case of Kr on free-standing graphene at 80 K finding no evidence of a commensuration between the two Kr monolayers. The flexibility of the graphene layer may have an important effect that will be addressed in future work.

We look forward to seeing reports of new measurements for noble gases on suppported and free-standing graphene and to be able to compare with our results.

Acknowledgement

We thank the financial support provided by the National Science Foundation, Center for Integrated Quantum Materials (CIQM), Grant No. DMR-1231319. We thank the financial support provided by the National Science Foundation, Partnership for Reduced Dimension Materials (PRDM), NSF Grant No. DMR1205608. We thank Milton Cole for his valuable comments on the manuscript.

References

[1] K.L. D'Amico, J. Bohr, D.E. Moncton, D. Gibbs, Melting and orientational epitaxy in argon and xenon monolayers on graphite, Phys. Rev. B 41 (1990) 4368–4376.
[2] Y. Larher, Triple point of the first monomolecular layer of krypton adsorbed on the cleavage face of graphite. Influence of the structure of this surface on the structure of the first adsorbed layer of rare gases, J. Chem. Soc., Faraday Trans. 1 (70) (1974) 320–329.
[3] A.D. Migone, Z.R. Li, M.H.W. Chan, Melting transition of submonolayer Ar adsorbed on graphite, Phys. Rev. Lett. 53 (1984) 810–813.
[4] Y. Larher, B. Gilquin, Critical temperatures of two-dimensional condensation in the first adlayer of noble gases on the cleavage face of graphite, Phys. Rev. A 20 (1979) 1599–1602.
[5] A. Thomy, X. Duval, J. Regnier, Two-dimensional phase transitions as displayed by adsorption isotherms on graphite and other lamellar solids, Surf. Sci. Rep. 1 (1981) 1–38.
[6] J. Unguris, L. Bruch, E. Moog, M. Webb, Ar and Kr adsorption on Ag(111), Surf. Sci. 109 (1981) 522–556.
[7] H. Taub, G. Torzo, H. Lauter Jr, S. Fain (Eds.), Phase Transitions in Surface Films 2, Plenum Press, New York, 1991.
[8] C. Ramseyer, C. Girardet, P. Zeppenfeld, J. Goerge, M. Büchel, G. Comsa, Xe monolayer adsorption on Cu(110): experiments and interaction calculations, Surf. Sci. 313 (1994) 251–265.
[9] M. Jaubert, A. Glachant, M. Bienfait, G. Boato, Uniaxial commensurate-incommensurate transition in surface films: Xe adsorbed on Cu(110), Phys. Rev. Lett. 46 (1981) 1679–1681.
[10] L. Bruch, M. Cole, E. Zaremba, Physical adsorption: forces and phenomena; Dover Publications, Mineola, 2007, Chapter 6.
[11] L.W. Bruch, M.W. Cole, H.-Y. Kim, Transitions of gases physisorbed on graphene, J. Phys.: Condens. Matter 22 (2010) 304001.
[12] L. Madeira, S.A. Vitiello, Properties of heavy rare-gases adlayers on graphene substrates, Surf. Sci. 655 (2017) 39–48.
[13] H.-Y. Kim, M.W. Cole, M. Mbaye, S.M. Gatica, Phase behavior of Ar and Kr films on carbon nanotubes, J. Phys. Chem. A 115 (2011) 7249–7257, PMID:21434679.
[14] H.-Y. Kim, E.C. Booth, M.T. Mbaye, S.M. Gatica, Contribution of chirality to the adsorption of a Kr atom on a single wall carbon nanotube, J. Low Temp. Phys. 175 (2014) 590–603.
[15] M.T. Mbaye, S.M. Maiga, S.M. Gatica, Commensurate phases of Kr adsorbed on single-walled carbon nanotubes, J. Low Temp. Phys. (2016) 1–9.
[16] D. Frenkel, B. Smit, Understanding Molecular Simulation: From Algorithms to Applications, Academic Press, 2001, Vol. 1.
[17] M. Calbi, M. Cole, S. Gatica, M. Bojan, J.K. Johnson, in: E. Bottani, J. Tascon (Eds.), Adsorption by Carbons, Elsevier Science, Amsterdam, 2008, Chapter 9.
[18] M.M. Calbi, M.W. Cole, S.M. Gatica, M.J. Bojan, G. Stan, Condensed phases of gases inside nanotube bundles, Rev. Mod. Phys. 73 (2001) 857–865.
[19] S. Gatica, M. Bojan, G. Stan, M. Cole, Quasi-one-and two-dimensional transitions of gases adsorbed on nanotube bundles, J. Chem. Phys. 114 (2001) 3765–3769.
[20] W.E. Carlos, M.W. Cole, Interaction between a He atom and a graphite surface, Surf. Sci. 91 (1980) 339–357.
[21] G. Stan, M.J. Bojan, S. Curtarolo, S.M. Gatica, M.W. Cole, Uptake of gases in bundles of carbon nanotubes, Phys. Rev. B 62 (2000) 2173–2180.
[22] G. Scoles, On the prediction of intermolecular forces between unlike atoms and molecules, Int. J. Quantum Chem. 38 (1990) 475–479.
[23] B. Smit, D. Frenkel, Vapor-liquid equilibria of the two-dimensional Lennard-Jones fluid(s), J. Chem. Phys. 94 (1991) 5663–5668.
[24] L. Bruch, M. Cole, E. Zaremba, Physical Adsorption: Forces and Phenomena, Dover Publications, Mineola, 2007.
[25] M. Bartolomei, E. Carmona-Novillo, M.I. Hernandez, J. Campos-Martinez, F. Pirani, Global potentials for the interaction between rare gases and graphene-based surfaces: an atom-bond pairwise additive representation, J. Phys. Chem. C 117 (2013) 10512–10522.